6.2 Potential Temperature, Salinity and Density (s_q) Distributions

In this section we shall present the general distribution of the classical oceanographic variables. For that purpose, and since the basic statistics are an important parameter which enables us to estimate the possible success of the EOF profile approach for shallower depths, we show the average and standard deviation profiles of the three basic variables, that is, potential temperature (frame (a)), salinity (frame (b)) and density (frame (c)), down to 500 m. In all these figures, the full lines stand for the statistics considering all the available data, while the dotted lines are considering the deep casts only. In frame (d) we show the number of data points used in the calculations.

We also present figures on the subsurface distribution (10 m depth) of density, and also some transversal sections. These two types of plots are performed with the gridded data after interpolation with the Successive Corrections (**SC**) methodology.

6.2.1 FANS I

The average and standard deviation curves (Figure 6-17) of potential temperature indicate that below 150 m the temperature distribution is nearly homogeneous all the way to the bottom, while the variability is concentrated, as expected, in the upper layer. While average temperature (and density) decrease (increase) linearly with depth from the surface down to less than 150 m, salinity increases gradually to greater depths (around 200 m).

The largest horizontal variability in all cases (represented by the standard deviation) is not found at the surface as one might expect (except in the case of salinity, where its values are similar); in fact, both density and potential temperature show two subsurface variability maxima. Just from the curves, it seems that the density distribution is controlled fundamentally by temperature and not by salinity, as is usually assumed in this particular region.

A last comment on this figure is on the similarity between the profiles obtained considering all the available data points and the ones estimated with the deep casts, which have previously been defined as those that reach depths of 500 m or deeper. The number of data points used to obtain the average and

standard deviation at each depth level are shown, as mentioned previously, in frame (d).º

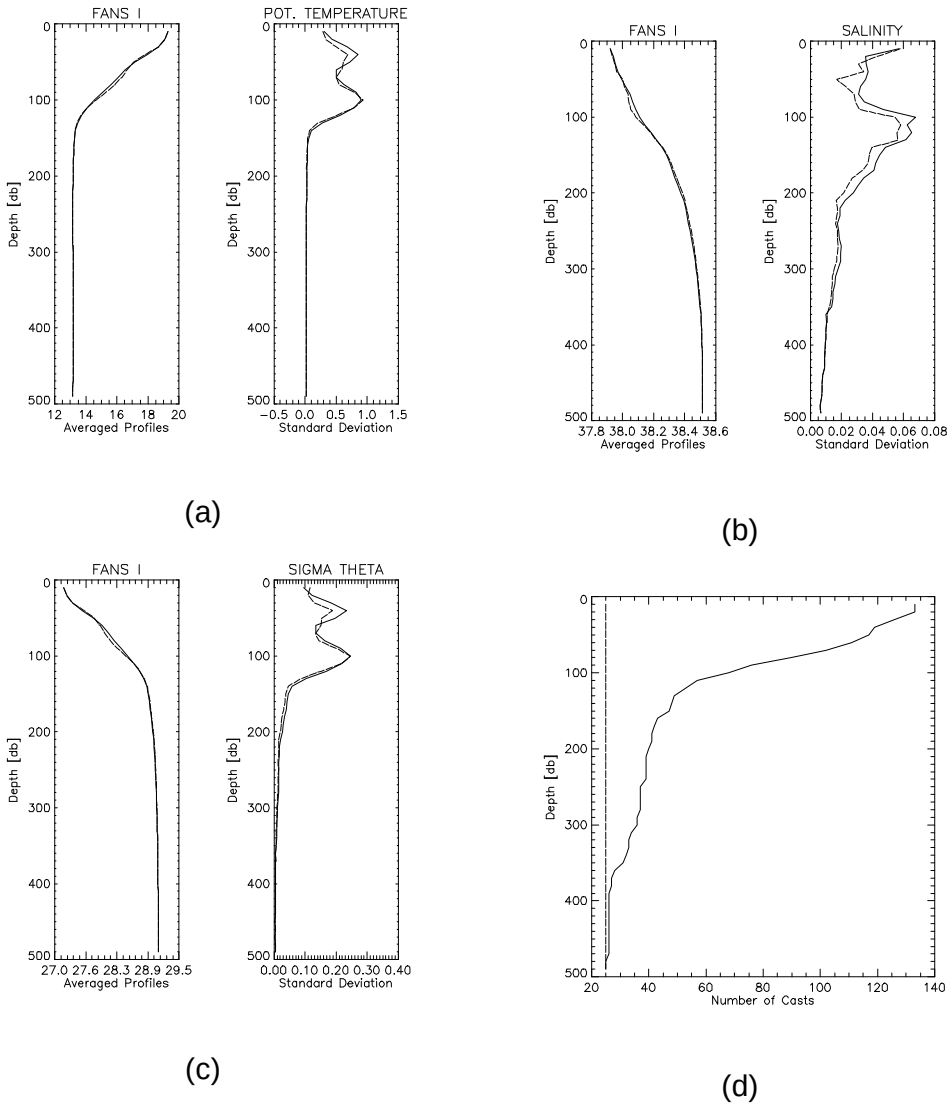

Figure 6-17. Average and standard deviation profiles for FANS I. The full lines represent the vertical distribution considering all the data, while the dotted lines stand for the profiles considering the deep casts only. Frame (d) shows the number of data points considered in the estimates.

Perhaps the most notorious feature observed in the horizontal subsurface density distribution (Figure 6-18) is the low density core at the north-eastern side of the domain. These low density values are reinforced both by the presence of warmer waters and lower salinities observed in this site. The second lowest density values are found surrounding the Ebro Delta, with the plume signal extending to the east.

The relative importance of potential temperature and salinity in the density field seems to be divided geographically (imaginary lines parallel to the north and south boundaries). At the northern third, salinity and temperature reinforce their effects, while south of the Ebro Delta, it is temperature which forces the density variability mostly (figures of temperature and salinity not shown). Finally, around the Ebro Delta, the effect of the lower salinities due to river discharge is somehow counterbalanced by the higher temperatures.

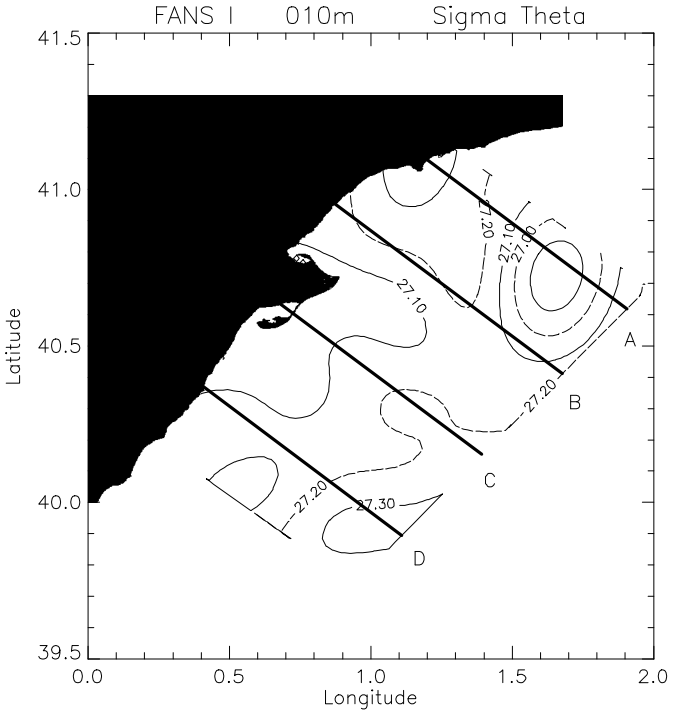

Figure 6-18 Density (Sigma Theta) contours at 10 m for the FANS I campaign. The four lines correspond to transects (A to D) to whom reference will be made in transversal section plots.

To give a general three-dimensional view of the density distribution, we include the contour plots of four transversal sections. The location of the transects is shown in the previous figure.

The FANS I campaign took place during autumn, and it is therefore in a transition stage from summer to winter conditions. This is reflected in the erosion of the pycnocline, which is not clearly identifiable as in the typical summer conditions. The process of mixing in the upper layer is clearly identifiable in transects C and D, in which there is not a vertical density gradient in the upper 30 m. In transects A and B, there is a clear downwards bending of the 28.4 isopycnal, and the ones below it, towards land.

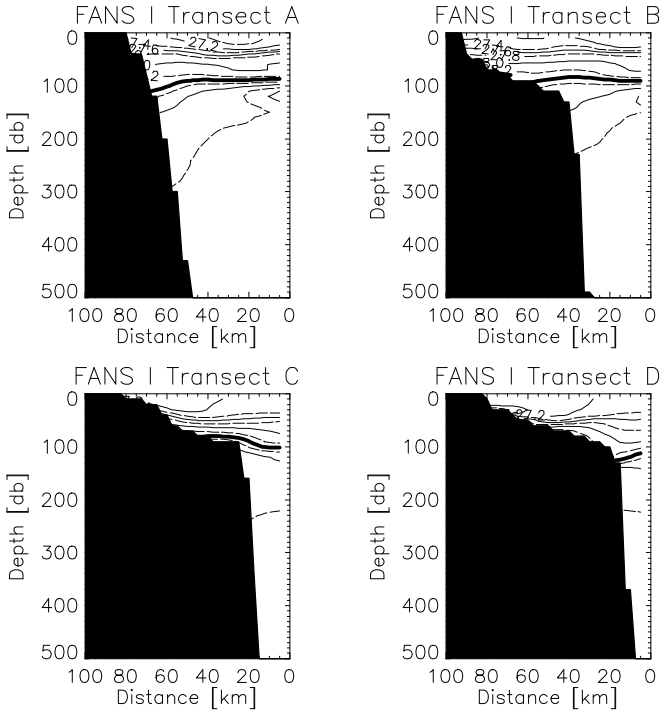

Figure 6-19 Density (sigma theta) transects for FANS I. The 28.4 isopycnal has been marked by a thick line. Successive isolines have a 0.2 difference.

6.2.2 FANS II

The basic statistics for this campaign can be found in Figure 6-20. The potential temperature average profile presents a range of less than one degree in the whole water column. It is also remarkably different from all the other campaigns, for it presents a surface inversion in which waters in the first 30 m (deep casts) or 100 m (all the casts) are colder than the waters below. As mentioned in the water masses section, this is fundamentally due to the large river runoff in this particular year. On the other hand, neither the salinity nor the density average profiles show any clear halocline or pycnocline, but their values tend to increase smoothly with depth.

The largest horizontal variability in all the variables is found at or near the surface, and from there the standard deviation profiles tend to decrease with depth.

Perhaps the greatest differences between the synthesis profiles obtained with all the casts and those computed with the deep casts only are found in temperature, and not so much in the numerical values (largest differences in

standard deviation slightly larger than 0.1), but in the general behaviour of the curves in the first 100 m.

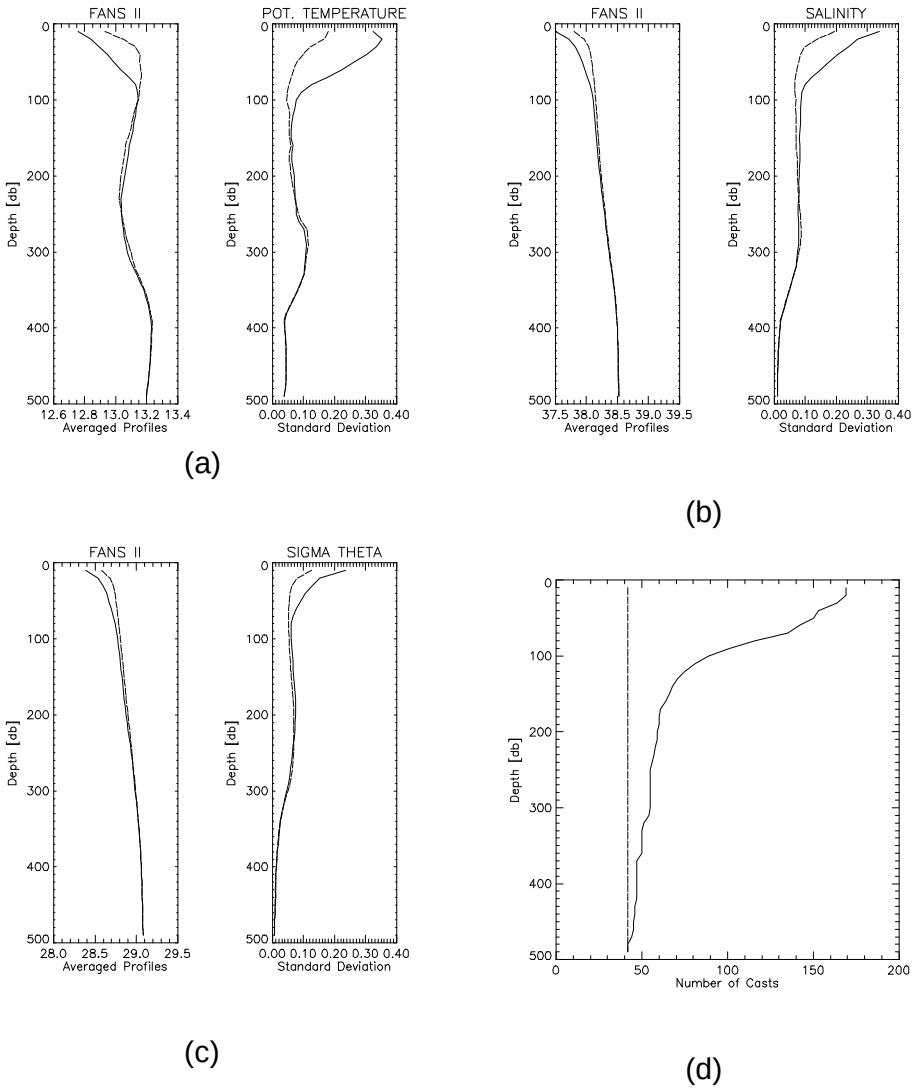

Figure 6-20. Average and standard deviation profiles for FANS II. The full lines represent the vertical distribution considering all the data, while the dotted lines stand for the profiles considering the deep casts only. Frame (d) shows the number of data points considered in the estimates.

Salinity dominates completely the subsurface density distribution all over the area. The lowest density values (Figure 6-21) are found in the river plume, which seems to be advected to the south. In general there are relatively low values all along the coast, while higher values are observed towards the slope that seem to have been advected from the north-east.

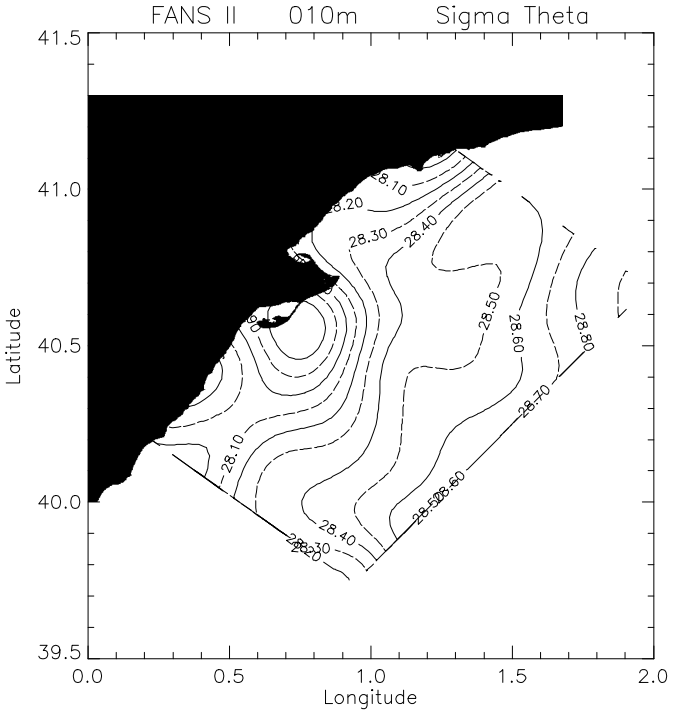

Figure 6-21 Density contours at 10 m for the FANS II campaign.

As mentioned previously, mesoscale activity in the Ebro region has been reported to be more intense during the winter months than in summer (Font et al., 1995) and the FANS II campaign took place in February. In the density cross-sections (Figure 6-22), the presence of a subsurface eddy becomes apparent in the northern section (transect A), which does not reach the Ebro Delta, but in the other sections there is a pronounced tilting of the pycnoclines which clearly indicates the existence of relevant horizontal density gradients, which in turn indicate the presence of enhanced geostrophic currents. These horizontal density gradients are intensified by the strong river outflows during the days previous to the campaign.

The presence of CIW (S < 38) is widespread in the subsurface layers, even down to 150 m in transect A (Figure 6-23. In this figure the 38 isohaline has been marked with a thicker line). Our understanding is that these low salinity waters in the northern section are not coming from the Ebro River, but have been advected from the north, together with the eddy whose presence is also clearly depicted in the salinity transversal section of transect A. We conclude the above because transect A is far enough to the north from the Ebro

Delta outflow, and since the northern current system flows towards the south, the presence of CIW at that location is more likely coming from the north. In fact, the largest fresh water supply in the north-western Mediterranean, and therefore the most important generator of enhanced density gradients during winter, is the Rhône River.

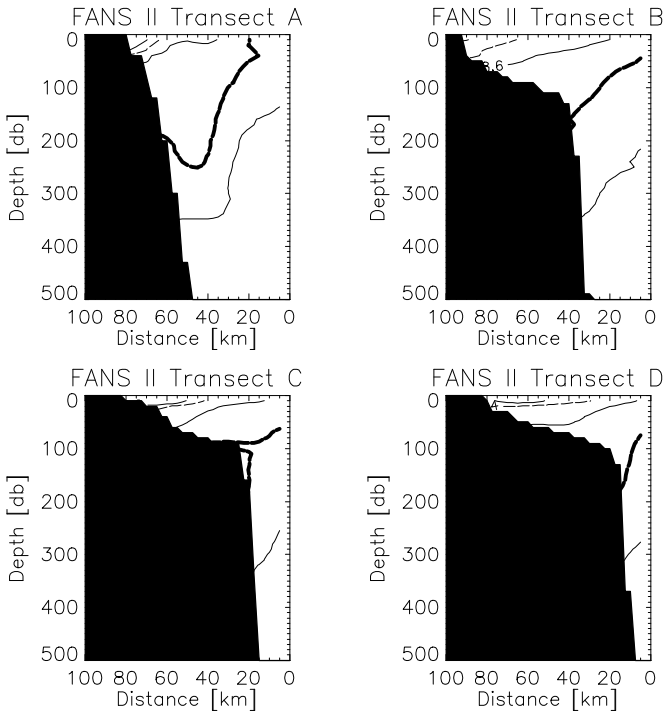

Figure 6-22 Four density (sigma theta) transversal sections during the FANS II campaign. The 28.8 isopicnal has been marked with a thick line; successive isolines have a 0.2 increment. Refer to Figure 6-18 for transect locations.

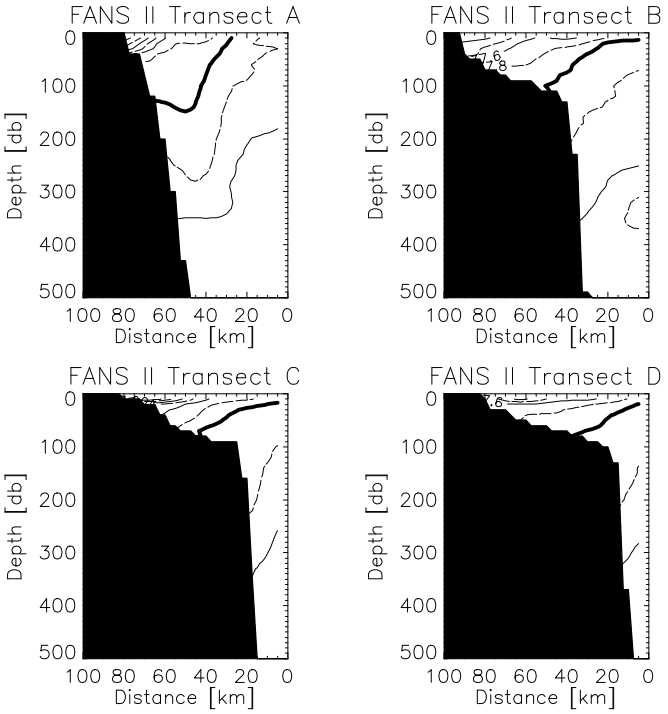

Figure 6-23 Salinity transversal sections during the FANS II campaign. The 38 isohaline is marked by the thick line, successive isolines differ in 0.2 units. Geographic location is the same as in the previous figure.

6.2.3 FANS III

The FANS III campaign (Figure 6-24) took place when summer conditions were nearly established, and the average temperature profile depicts clearly the depth of the thermocline at 40 m. In this depth range, temperature decreases from 22^{o}C at the surface to 15^{o}C. This gradient is also evident in density, with profiles that clearly mirror the temperature vertical distribution and the pycnocline is located at the same depth as the thermocline. As for salinity, the average profiles decrease, like in the previous campaigns, gradually with depth.

As in FANS I, the horizontal variability is not greatest at the surface (except in salinity considering all the casts) but rather at a depth of 20 or 30 m, and this peculiar behaviour can not be attributed to continental influence for it is also present in the profiles considering the deep casts only. This could be the result of a mixing process, which would tend to homogenize the variability, and the most probable agent is the wind, which can affect the upper layer.

There are no significant differences between the profiles obtained with all the casts and with the deep ones only; in fact, the average profiles are nearly identical.

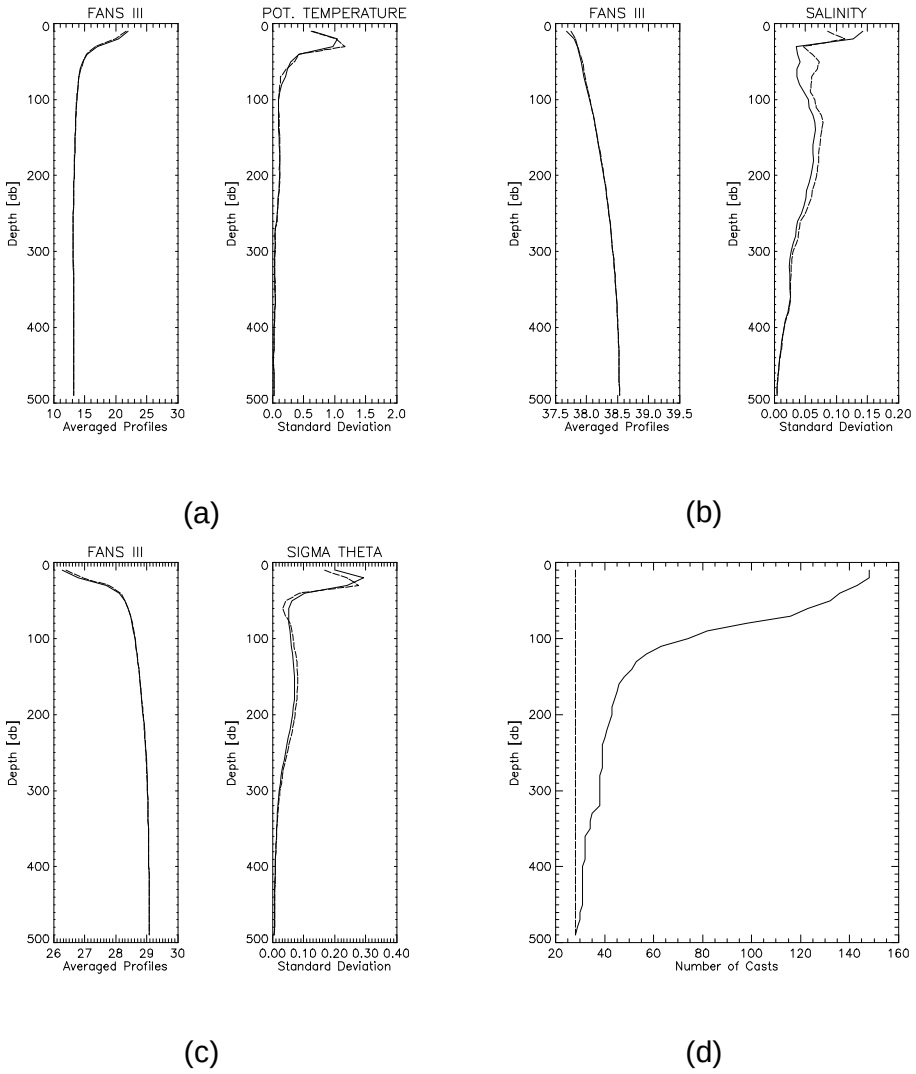

Figure 6-24. Average and standard deviation profiles for FANS III. The full lines represent the vertical distribution considering all the data, while the dotted lines stand for the profiles considering the deep casts only. Frame (d) shows the number of data points considered in the estimates.

In general terms, we could view the density subsurface distribution (Figure 6-25) as increasing from the south-west to the north-east. The strongest gradient is found in the south-west, adjacent to the coast, and its structure coincides both in the temperature and salinity distributions, which oppose their

effects on density (higher temperatures, but lower salinities). This feature is likely due to the intrusion of waters coming from the Gulf of Valencia, with a more recent Atlantic origin.

And while the Ebro River plume is very well observed in the salinity distribution, there is no sign of it in temperature. This results in a mild density signature of the plume.

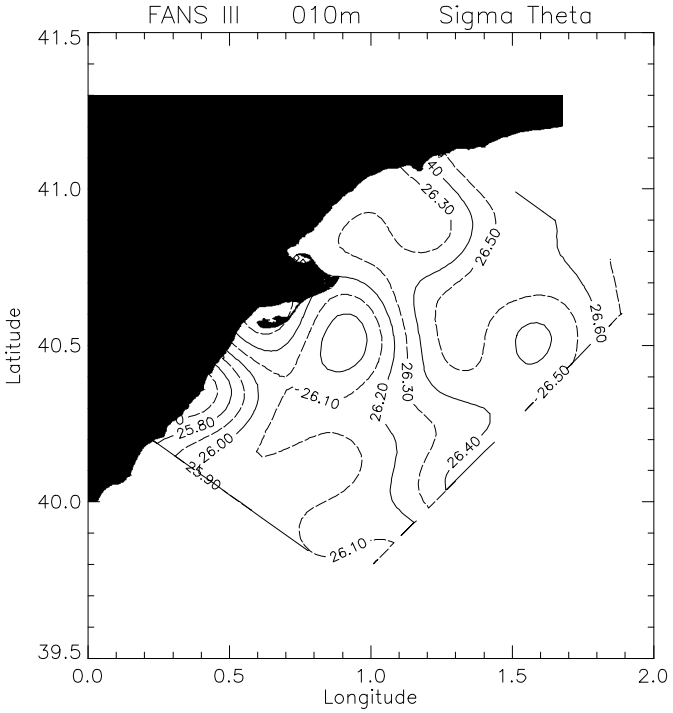

Figure 6-25 Density contours at 10 m for the FANS III campaign.

The transversal sections of density (Figure 6-26. In it, successive contour intervals have an increment of 0.5 instead of 0.2 as in the rest of similar figures) depict clearly the pycnocline at around 50 m depth, with a value of 28 kg/m^3 (σ_θ). Comparing it to its equivalent figure for the FANS II campaign (Figure 6-22), there are evident differences, such as a larger range of values in FANS III due to the effects of higher temperatures which make the waters lighter, and a less pronounced tilting of pycnoclines that results in lower horizontal gradients, hence in less intense geostrophic currents.

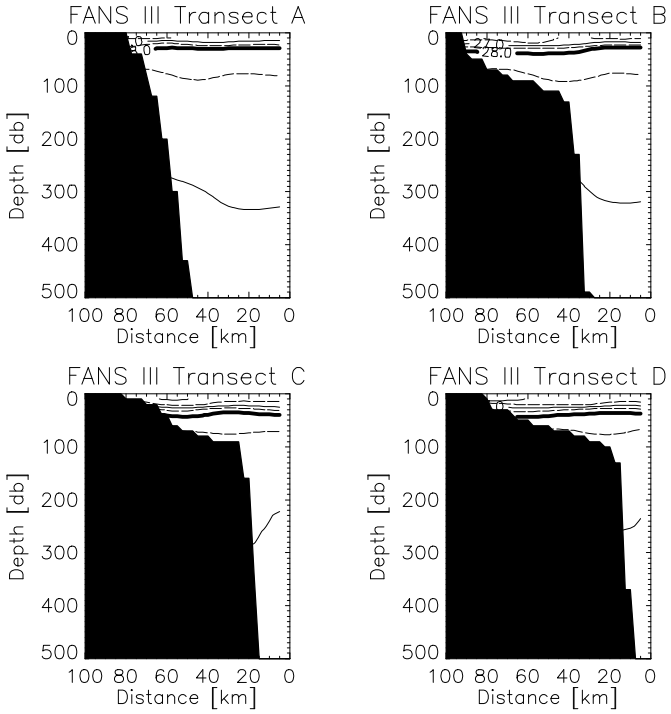

Figure 6-26 Density (sigma theta) transects for FANS III. The 28 isopicnal has been marked by a thick line. Successive isolines have a 0.5 increase instead of 0.2, which is the case for all the other similar plots.

6.2.4 MEGO 94

The MEGO 94 campaign (Figure 6-27), as FANS II, took place during winter, and the temperature range of the average profiles is slightly less than one degree. In this campaign there is no average temperature inversion in the upper layer; in fact the average temperature decreases form 13.1^{o}C to 12.5^{o}C at 40 m. From this depth level, it remains constant until at around 170 m depth, where it increases again. This mixed intermediate layer with nearly constant average values is also present in salinity and density. If we consider the average salinity estimated with the deep casts only, then this homogeneous layer starts at the surface. One interesting aspect of this campaign is the fact that the deep relative temperature maximum, which indicates the depth of the core of the LIW layer, is found at around 500 m, that is more than 100 m deeper than in the FANS campaigns.

The horizontal variability is greatest at the upper layer if we consider all the available data, particularly in salinity and density. But if we consider the

deep casts only, then the previous variables have its largest variability at around 300 m, but even those values are relatively small, which means that during this campaign, the average conditions reflect rather homogeneous conditions except in the first 50 or 60 m.

MEGO 94 is the campaign in which we meet the largest differences in the upper layer between the variables when we consider all the available data for the statistical estimates, particularly the standard deviation, or the data from the deep casts only. This fact is important when we try to apply the EOF's methodology as an extrapolation method to shallower regions. Another important factor is the fact that while there is a larger number of casts, and a closer sampling of the Ebro Delta region, the number of deep casts is only 25.

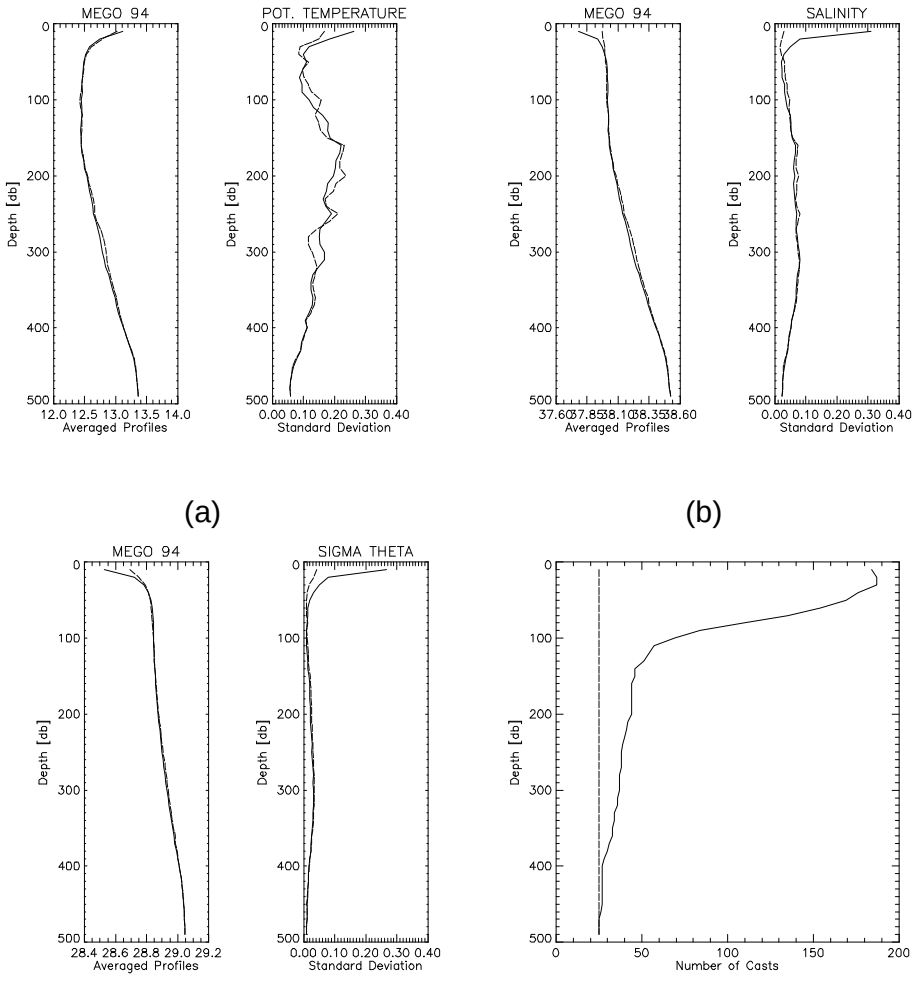

Figure 6-27. Average and standard deviation profiles for MEGO 94. The full lines represent the vertical distribution considering all the data, while the dotted lines stand for the profiles considering the deep casts only. Frame (d) shows the number of data points considered in the estimates.

As in FANS II, the overall subsurface density distribution (Figure 6-28) is clearly controlled by salinity, for the temperature range is less than one degree. There is a very homogeneous distribution in the whole domain, particularly in the northern third of the area, and practically all the structure observed is associated to the Ebro Delta plume. In general, the conditions under which the campaign took place were apparently very calm from the dynamic point of view, with little structure both in the horizontal and in the vertical (Figure 6-29).

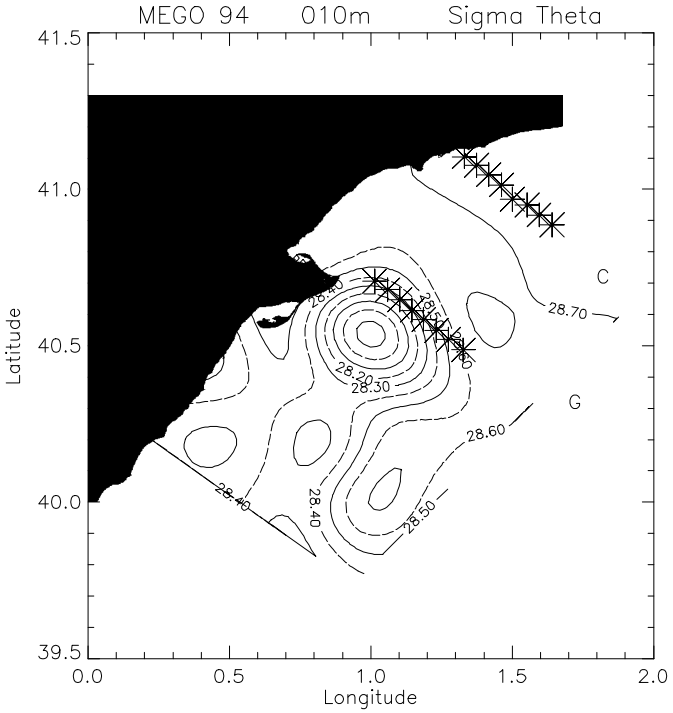

Figure 6-28 Density contours at 10 m for the MEGO 94 campaign. The stars mark the cast position of three different transects. From north to south: C, G and L.

The density transversal sections show clearly the difference between a northern section with little structure (transects A and B), and a southern one with slightly more variability due to the Ebro Delta outflow (Transect C).

The remarkable difference between this campaign and FANS II, both carried out during the winter months, simply reflects the inter-annual variability and the complexity of the study area from the geophysical point of view.

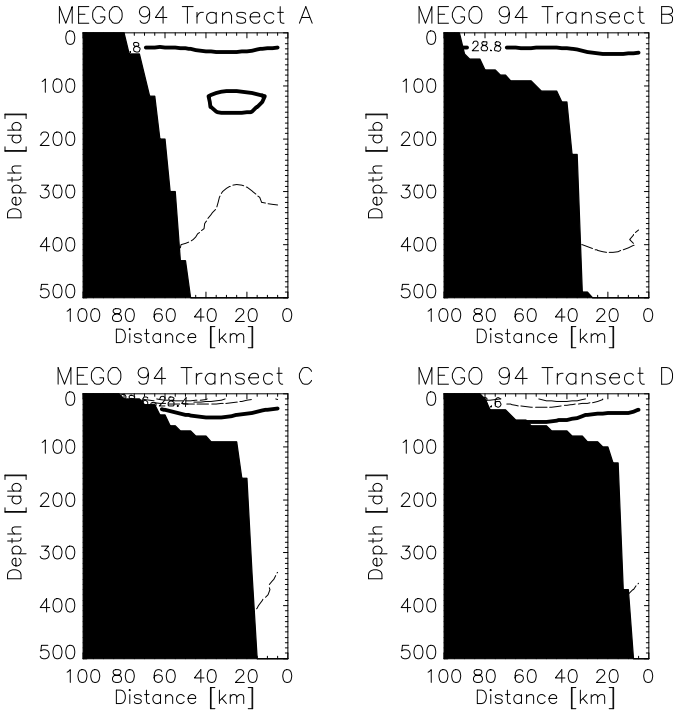

Figure 6-29 Density transversal sections during MEGO 94 campaign. The 28.8 isopicnal has been marked with a thick line; successive isolines have a 0.2 increment.

6.2.5 Historic Data – Summer Conditions

As mentioned previously, in order to evaluate the potential use of historic data EOFs as an extrapolation method for shallower regions, we used the basic statistics and eigenvectors obtained from 188 deep casts. We now present the average and standard deviation profiles obtained from these deep casts (dotted lines as in the previous plots), and also the profiles obtained from all the available casts.

At first sight, the similarity between both the average and standard deviation profiles from all the casts and the deep ones only is remarkable (Figure 6-30). This is even more surprising when we consider the number of data points used in the estimates (frame d), from 658 in the upper layer and decreasing with depth, to 188 deep ones.

The average temperature decreases smoothly from 19.5^{o}C at the surface to around 13^{o}C at 80 m, and from there remains constant. This behaviour also

applies to the standard deviation profile, but its values tell us that the horizontal variability is significant in the upper layer, with more than 3^{o}C near the surface.

The average salinity increases with depth, but there is no intense halocline. The average salinity is nearly constant below 300 m depth. Its horizontal variability has maximum values at the surface as one might expect, and decreases gradually down to 300 m depth, though in a less pronounced way than in the upper 80 m.

There are clear differences in distribution, particularly in the standard deviation, between the historic summer data profiles and the campaign ones. The differences in range are easily explained by the larger geographic area considered for the historic data. FANS III, which took place during summer or nearly summer conditions (refer to figure Figure 6-24), has a slightly larger surface average temperature and a slightly shallower depth for the thermocline, and the standard deviation maximum is not at the surface. The salinity average profiles are very similar (x-axis with different ranges) but not so the standard deviation profiles. Finally, the density of the historic data reaches values significantly higher at depth.

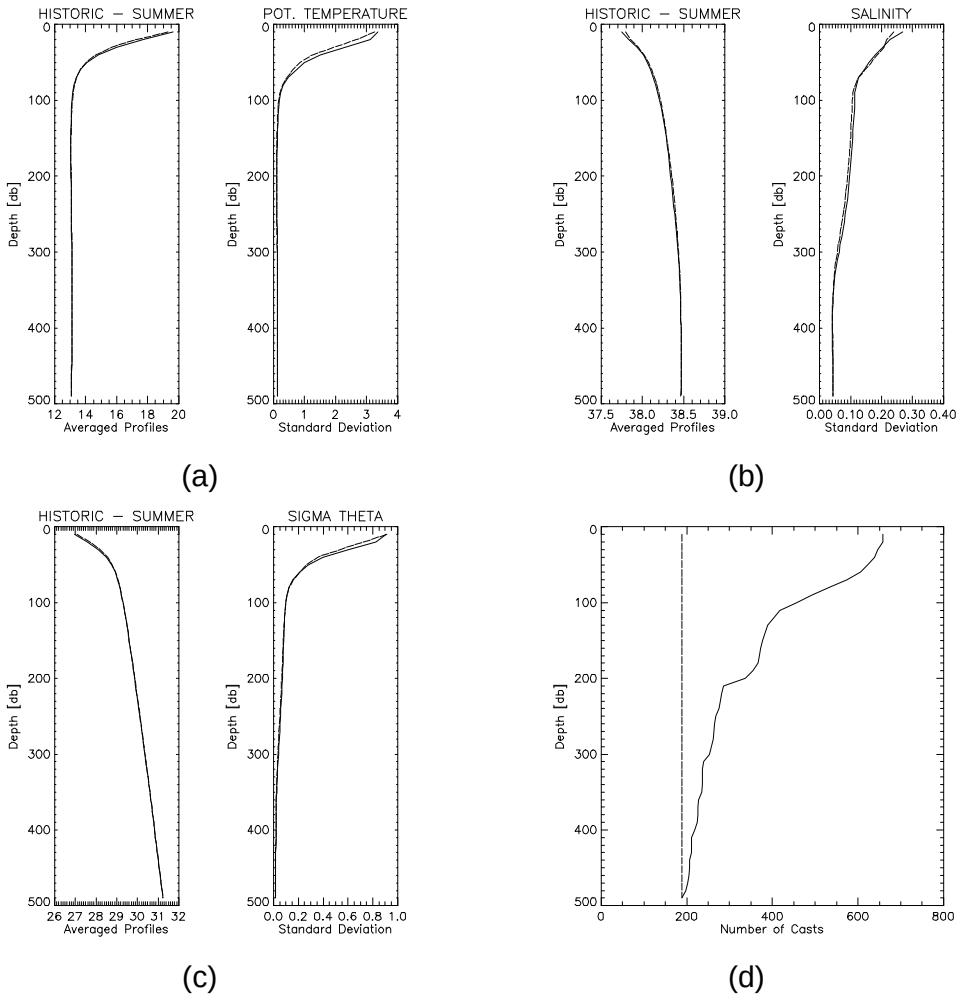

Figure 6-30 Average and standard deviation profiles obtained with the Historic Summer Data. The full lines represent the vertical distribution considering all the data, while the dotted lines stand for the profiles considering the deep casts only. Frame (d) shows the number of data points considered in the estimates.

6.2.6 Historic Data – Winter Conditions

The available CTD casts for winter are significantly less than for summer, 308 cast in total, of which only 85 casts are deep. The eigenvectors and statistics of these latter ones are used to test the extrapolation method.

The whole average potential temperature range is significantly larger (4^{o}C) than the observed during FANS II and MEGO 94 (less than 1^{o}C), and no inversion as in FANS II is observed. The average temperature considering all

the casts decreases from 17^{o}C at the surface to 13^{o}C at around 90 m depth, and from 15^{o}C to 13^{o}C; from there on it remains nearly constant with depth. Both profiles present a similar standard deviation, which means that the average horizontal variability is nearly the same. On the other hand, the average salinity profiles decrease rather smoothly from the surface to around 200 m, and from there on it remains nearly constant. There is a slight difference towards lower values in the profile obtained with the deep casts only down to 400 m. The average horizontal variability decreases with depth, and there is not a significant difference between both profiles. The average density increases with depth at a nearly constant rate for levels deeper than 60 m, but in a slightly stronger way in the upper 50 m layer, specially if we consider all the available casts. The average horizontal variability decreases significantly from the surface to 90 m depth, and from there continues to decrease at a lower rate, without any significant difference between the profiles obtained with all the casts and with the deep ones.

It is interesting to notice that at 500 m depth, the average density profiles obtained with the historic data, both for summer and winter, reach values exceeding 31 kg/m^3 (σ_θ) while during the FANS and MEGO campaigns the largest density was 29.1. This is easily explained by the location of the historic data, which include stations outside our particular study domain, particularly to the north (refer to the corresponding figures in chapter 5).

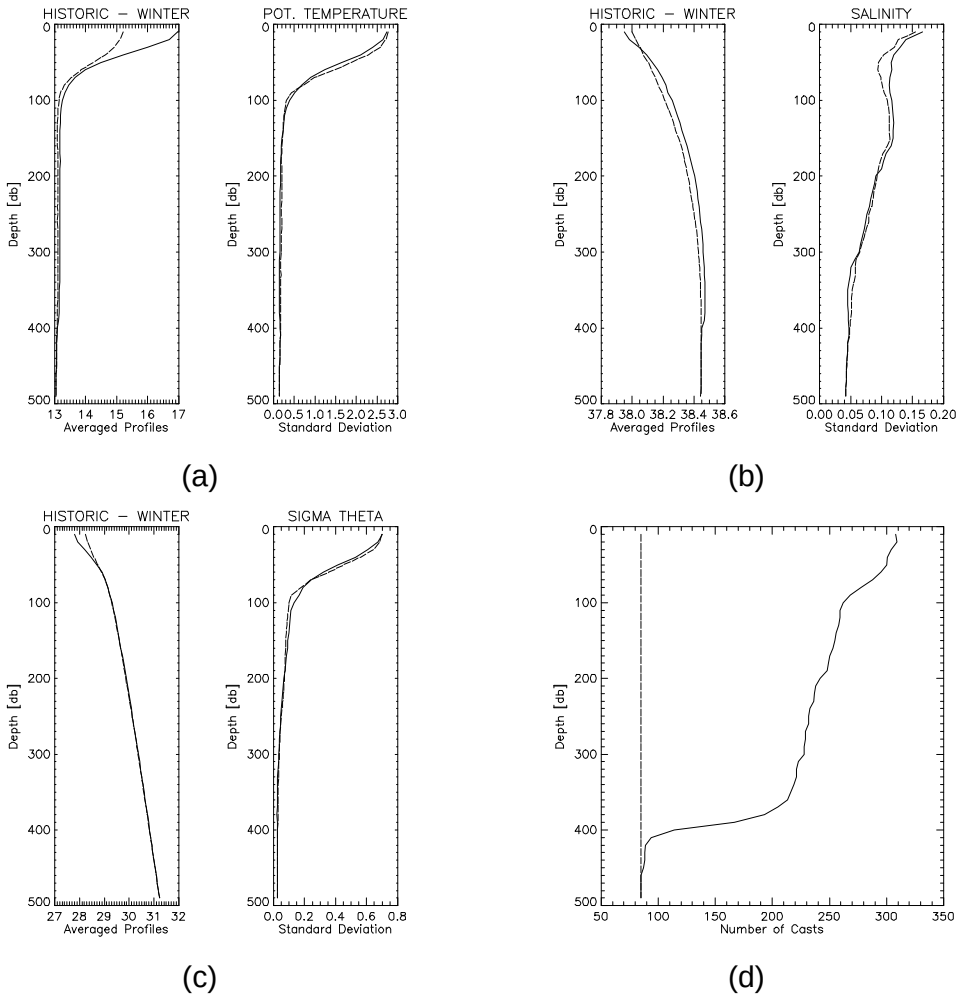

Figure 6-31 Average and standard deviation profiles obtained with the Historic Winter Data. The full lines represent the vertical distribution considering all the data, while the dotted lines stand for the profiles considering the deep casts only. Frame (d) shows the number of data points considered in the estimates.

6.3 Dh Distributions

As mentioned before, one of the goals of the present research is the analysis and comparison of the geostrophic currents in a shelf/slope area obtained through two different methods: the one proposed by Csanady in 1979 and another one based on EOF's analysis.

The basic theory on geostrophic currents is presented in Chapter 7. In fact, dynamic height represents the pressure field at a given depth assuming that there is a deeper level in which isobars are perfectly horizontal (i.e. a level

without any horizontal gradients which could induce a current). From this assumed level of no motion, a vertical integration can be carried out upwards to derive geostrophic currents at any given level.

Bearing thus in mind that the horizontal gradients of dynamic height (which has units of energy per unit mass) are directly related to the magnitude of geostrophic currents, the statistical parameter which could signal the intensity of these currents is the standard deviation; but in fact, it can only serve as a rough indicator, for the same standard deviation value could be obtained for a horizontal distribution in which there is one particular region with a strong gradient and for another in which the variability is homogeneously distributed throughout the study area.

With the above idea in mind, we present the average and standard deviation profiles (Figure 6-32) of dynamic height (in dynamic centimetres) for the four campaigns. In these figures there is only one set of synthesis profiles, for the dynamic heights have been computed only with data from the deep casts.

There are similarities in the average profiles between FANS I and FANS III, and between FANS II and MEGO 94. In the first case there is a clear curvature towards higher values (x axis is negative in all plots) in the upper 100 m, and below that depth profiles increase linearly to zero. In the second case, the average profiles increase linearly from the surface down to 500 m depth.

The standard deviation curves suggest stronger geostrophic currents at around 20 or 30 m in FANS I, and around 50 m in FANS III. On the other hand, the largest horizontal gradients might be found at the surface in FANS II and MEGO 94; even though the profiles do not differ significantly in these winter campaigns, the magnitude in MEGO 94 is significantly smaller than in FANS II. This last fact reinforces what was written before about the little variability and weak dynamics observed in MEGO 94.

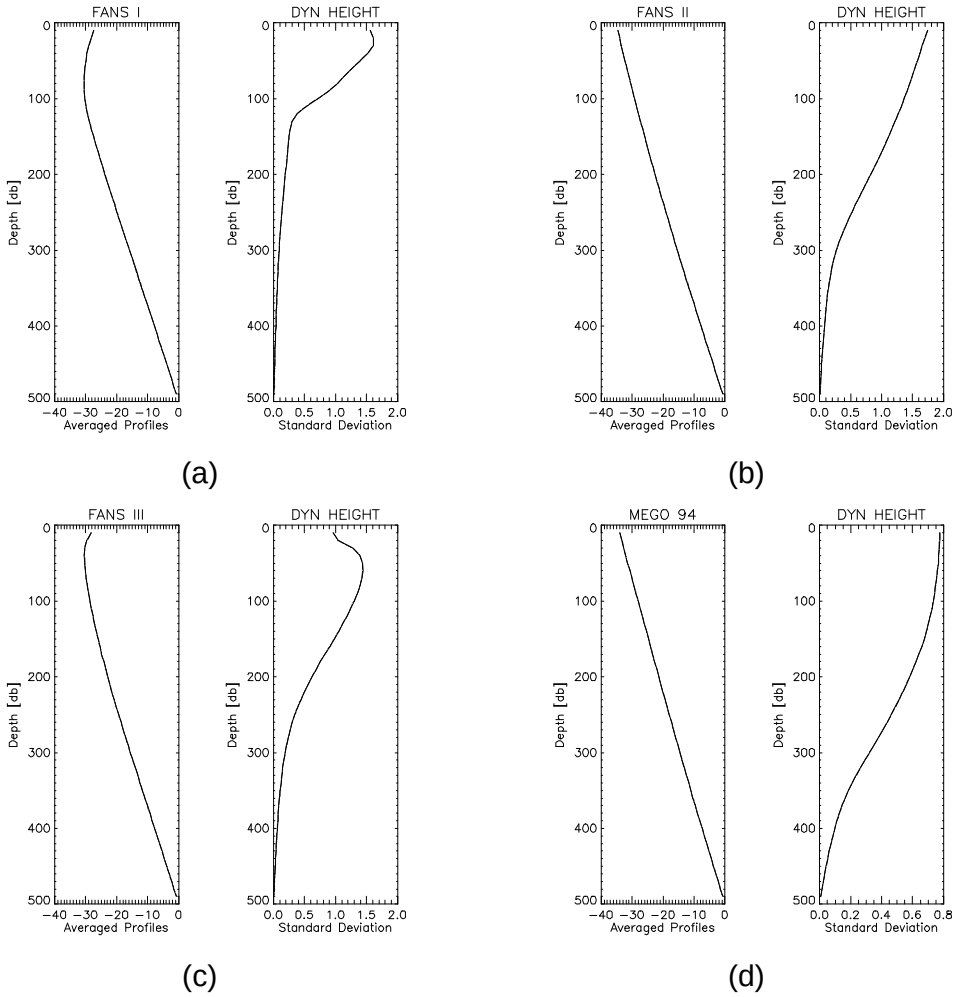

Figure 6-32 Average and standard deviation profiles of dynamic height (in dynamic centimetres) for the four campaigns. FANS I (a), FANS II (b), FANS III (c) and MEGO 94 (d). The number of deep casts used in the estimates are, respectively: 25, 25, 42 and 28.

In Figure 6-33 we present the dynamic height contours at 10 m for all the campaigns, with an additional figure (frame d) at 50 m for FANS III. This one was included to check weather the maximum in the standard deviation corresponded, in fact, to larger gradients. In this particular case it does reflect the above situation. These contours were generated with the deep casts data, where the vertical integration from the assumed level of no motion (500 m) was performed, and the results were further interpolated through the SC procedure. The shaded area in the figures corresponds to depths shallower than 500 m.

Since larger gradients in dynamic height are directly proportional to the geostrophic current speed, the dynamic height distribution enables us to

conclude that the stronger currents took place during the FANS II campaign (frame b), where the northern current appears very well established in its south-westward flow. During FANS I (frame a), the northern current appears in the north-eastern area, and its signal seems to be broken by an across shelf structure in the middle of the domain. On the other hand, the dynamic height distribution during FANS III (frames c and d) indicates little velocities in the north-east and an across shelf structure in the middle of the domain, which is stronger at 50 m than at 10 m, and again a south-western flow in the south. Finally, the distribution in MEGO 94 (frame e) could indicate the partial presence of two cyclonic structures.

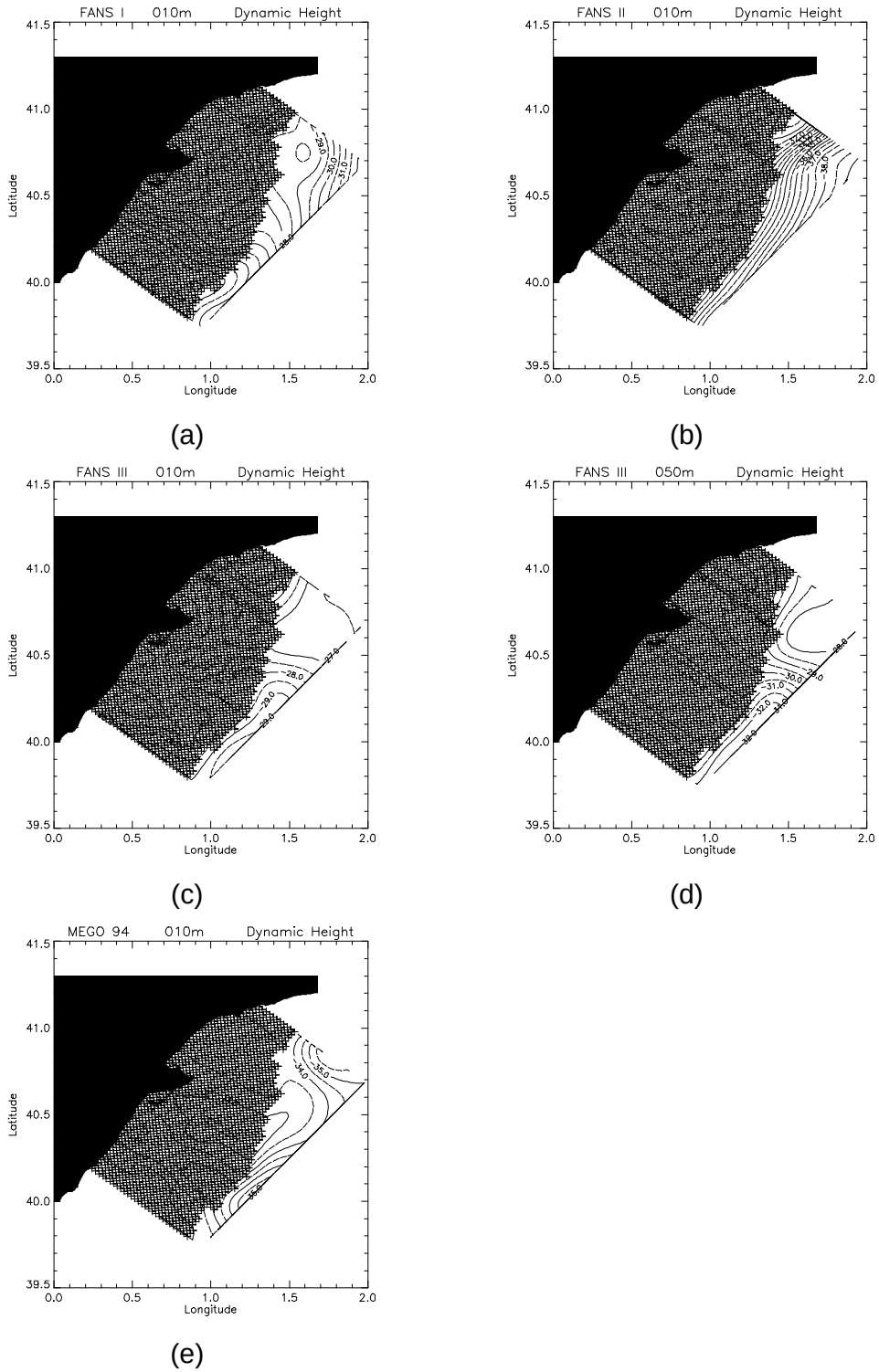

Figure 6-33 Dynamic height contours (in dynamic centimetres) at 10 m (with the additional figure for FANS III at 50 m) for the four campaigns. FANS I (a), FANS II (b), FANS III (c and d, the latter at 50 m) and MEGO 94 (e).